NJC

Check for updates

Chitosan as a solid catalyst for the one-pot Knoevenagel condensation in the context of sustainable chemistry

Usman Ali, [ID] [ac] Friedemann Dressler, [ID] [b] Lysander Q. Wagner, [ID] [ac] Paul P. Debes, [ID] [ac] Jaime Gallego, [ac] Peter R. Schreiner [ID] *[bc] and Bernd M. Smarsly [ID] *[ac]

We employed chitosan to catalyse the Knoevenagel condensation between various benzaldehydes and ethyl cyanoacetate. Chitosan exhibited excellent reusability, maintaining catalytic efficiency over six reaction cycles with yields consistently between 95% and 98%, for benzaldehyde and *p*-tolualdehyde. Furthermore, we were able to recycle the used solvent (ethanol), enhancing overall sustainability. Expanding the application of chitosan, we synthesised 4-methyl-3-oxo-*N*-phenyl-2-(phenylmethylene)-pentanamide, a key intermediate of the statin drug Atorvastatin synthesis on gram-scale with 96% yield. This demonstrates the use of chitosan as a catalyst for the synthesis of fine chemicals with improved sustainability; notably, the chitosan-catalysed process aligns with several key principles of sustainability. The employed chitosan exhibited a high water-binding capacity of about 520%, which enhances product formation by capturing water as the reaction byproduct. The high yields in the repeated use originated from the catalytic action of a large number of amino groups and the extraordinary and reversible swelling and binding capacity for polar solvents. We propose that such a swellable, insoluble, abundant catalyst material that is able to bind large amounts of water, constitutes a promising concept in organocatalysis. Analytical techniques such as scanning electron microscopy, mercury intrusion porosimetry, diffuse reflectance infrared Fourier transform spectroscopy, and X-ray diffraction analysis verified the catalyst's integrity, showing no significant physical or chemical degradation after multiple uses. Thus, chitosan emerges as a sustainable catalyst for organic synthesis with promising implications for Knoevenagel reactions.

Introduction

Natural biopolymers are increasingly explored as supports or active components in the design of sustainable heterogenous catalysts for organic synthesis.[1–3] The underlying principles include the development of environmentally friendly processes that reduce waste, minimize energy consumption, and utilise renewable resources.[4,5] A sustainable heterogeneous catalyst for organic synthesis must exhibit high catalytic efficiency, stability, reusability, and ideally biodegradability. For example, mesoporous silica-supported catalysts and polymer-supported organocatalysts are known for their high efficacies and selectivities, but immobilization of organocatalysts on different supports frequently involves hazardous solvents, acids, or bases.[6–10] The use of natural biomolecules and biopolymers as organocatalysts for organic reactions can be considered a particularly appealing concept for sustainable organic transformations due to their abundance, biocompatibility, chiral backbones, and biodegradability.[2,11]

Chitosan is such an example, composed of poly-D-glucosamine, and it is abundantly available in living organisms.[12] Technically, chitosan is obtained by deacetylation of chitin, which is a poly-*N*-acetylglucosamine extracted from the exoskeleton of shrimp, crabs, and a few molluscs (Fig. 1).[13,14] The unique features of chitosan as a solid heterogeneous catalyst, among others, are its natural abundance, biocompatibility, and enormous number of amino groups in the backbone.[15–17] Amino groups act as catalytic sites for base-catalysed organic reactions, but can also be transformed into other functional groups. For instance, the chitosan amino groups can be converted into imines by reaction with aldehydes, to use them, for example, as anchoring sites of metal complexes.[18,19]

[a] Institute of Physical Chemistry, Justus Liebig University, Heinrich-Buff-Ring 17, 35392 Giessen, Germany. E-mail: bernd.smarsly@phys.chemie.uni-giessen.de

[b] Institute of Organic Chemistry, Justus Liebig University, Heinrich-Buff-Ring 17, 35392 Giessen, Germany. E-mail: prs@uni-giessen.de

[c] Center for Materials Research, Heinrich-Buff-Ring 16, 35392 Giessen, Germany
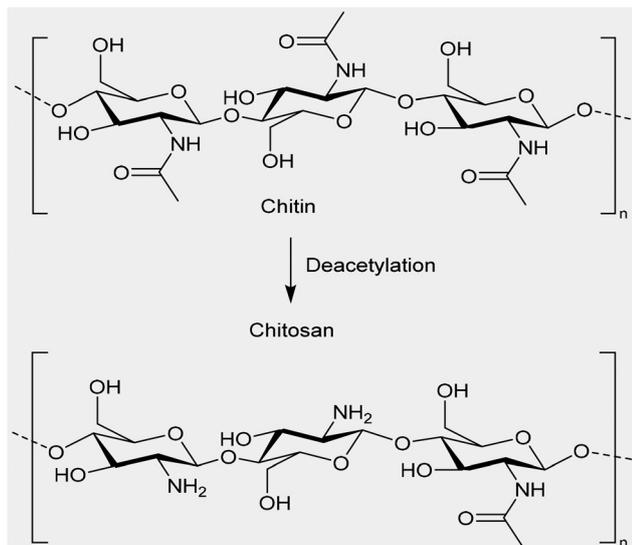
Fig. 1 Deacetylation of poly-*N*-acetylglucosamine (chitin) to poly-*d*-glucosamine (chitosan).

So far, materials widely used as a heterogeneous catalyst for base-catalysed organic reactions are porous silica materials, zeolites, and metal organic frameworks (MOFs) containing amino groups.[6,20–23] Among amino-functionalized silica, zeolites, or MOFs, chitosan is considered to be superior in terms of sustainability and natural availability, as it is derived from chitin, which is the second most abundant biopolymer after cellulose.[24–27] Typical uses of chitosan as a basic heterogeneous catalyst or as a support for anchoring metals concern micro- and nano-scaled particles, flakes, fibres, sponges, gel beads, and membranes.[28–33]

In 2017, Sakthivel *et al.* first reported the use of pristine chitosan as a solid base catalyst for the Knoevenagel condensation to synthesize benzylidenemalononitriles. They achieved high yields with different benzaldehydes and malononitrile under mild conditions (40 °C, ethanol, solvent) and demonstrated chitosan's reusability for up to four cycles without significant loss in activity.[28]

In 2020, Anbu *et al.* expanded on this by using chitosan for the Knoevenagel–Doebner condensation to synthesize α,β-unsaturated carboxylic acids. They conducted reactions at 70 °C, testing various solvents, and found no loss in catalytic activity over five cycles, together with no significant structural changes in chitosan as confirmed by XRD and SEM analysis.[26] Later in 2020, Anbu *et al.* extended their work to Knoevenagel condensations of benzaldehydes with cyanoacetamide, once again showing stable catalytic performance over five cycles with no structural and changes in chitosan.[25]

While the general mechanism of the Knoevenagel reactions, involving aldehydes and NH$_2$ groups as catalyst, is well known, a few studies addressed mechanistic details and revealed the relevance of the stability of the imine intermediate for the product formation, using DFT calculations and suitable NMR experiments.[34,35]

Despite these promising results, several challenges persist. Previous studies relied on hazardous solvents such as DMF, DMSO, or DCM, which are incompatible with green chemistry standards. Additionally, high reaction temperatures (*e.g.*, 70 °C) and the absence of solvent recycling reduce the overall sustainability of the processes. Moreover, research on gram-scale synthesis and applications in industrially relevant reactions particularly for drugs preparations *etc.* have not been reported. The sustainability claim is limited to the use of solid chitosan or chitosan derivatives as sustainable catalyst, while the broader principles of green chemistry are not consistently applied throughout the process.[25,26,35,36] To address these challenges, we focused on the use of solid chitosan as a catalyst for Knoevenagel condensations, discussing potential industrial relevance. While previous studies demonstrated chitosan-catalysed Knoevenagel condensations, *e.g.*, using malononitrile (p$K_a \approx 11.0$ in DMSO at 25 °C) and cyanoacetamide (p$K_a \approx 9.0$),[25,26] our study uses ethyl cyanoacetate (p$K_a \approx 13.1$), a less acidic and sterically more demanding substrate.[37] Thus, ethyl cyanoacetate is used to clarify if chitosan shows promising catalytic performance also for a compound with lower C–H acidity under mild conditions, especially room temperature. In particular, after exploring the reaction of benzaldehydes with ethyl cyanoacetate as a model and we extend our study to the synthesis of an Atorvastatin intermediate [4-methyl-3-oxo-*N*-phenyl-2-(phenylmethylene)pentanamide] with improved sustainability with respect to several criteria. Atorvastatin is a widely used statin drug for preventing cardiovascular diseases, and its efficient synthesis is of significant pharmaceutical relevance.[38–41]

Compared to previous studies on chitosan used for the Knoevenagel reaction, our study focuses on "green chemistry" principles by utilizing eco-friendly solvents like ethanol and acetone, employing conditions near room temperature, and facilitating catalyst and solvent recovery to minimize waste.

Additionally, chitosan's remarkable affinity for water is studied by water-binding capacity (WBC) and water vapour sorption studies. This unique property enables chitosan to capture the water produced in the Knoevenagel condensation, effectively driving the reaction toward condensation. Moreover, chitosan's significant swelling capacity for the employed solvent ethanol is believed to enhance the accessibility of catalytic sites, highlighting its adaptability as catalytic systems.

To assess the robustness of the catalyst, we conducted detailed analyses using scanning electron microscopy (SEM), mercury intrusion porosimetry (MIP), diffuse reflectance infrared Fourier transform spectroscopy (DRIFT), and X-ray diffraction (XRD).

Thus, our study addresses and discusses the sustainable use of chitosan as a solid base catalyst for fine chemical synthesis. By aligning with green chemistry principles, our study is intended to contribute to the development of eco-friendly and more efficient organocatalytic processes.

Results and discussions

Efficiency of chitosan as solid catalyst for Knoevenagel condensations

Here, we focus on the Knoevenagel reaction between benzaldehydes and ethyl cyanoacetate (Scheme 1) as our standard
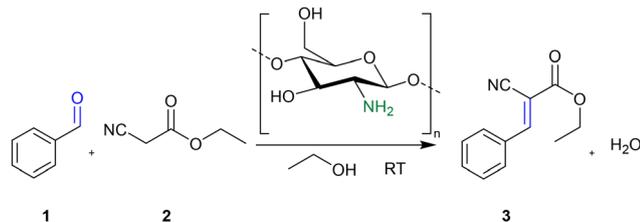
Scheme 1 Knoevenagel condensation of benzaldehyde with ethyl cyanoacetate at room temperature using solid chitosan as catalyst in ethanol.

Table 1 Optimization of reaction parameters for the reaction between benzaldehyde (**1**) and ethyl cyanoacetate (**2**) at room temperature[a]

Entry	Chitosan[b] (mg)	Time (h)	Yield (%)
1	0	72	$<1^c$
2	0^d	48	<3
3	25	24	45
4	50 1st run	24	93
5	50 2nd run	24	95
6	50 3rd run	24	95
7	50 4th run	24	96
8	50 5th run	24	96
9	50 6th run	24	96
10[e]	50	13	94
11	100	20	95

[a] Reaction conditions: 2 mmol benzaldehyde and 2 mmol ethyl cyanoacetate in 2.5 mL EtOH at 25 °C. [b] 50 mg of chitosan reused six times, no loss in catalytic activity observed. [c] Blank reaction analysed with GC. [d] 50 mg of chitin used instead of chitosan to analyse the influence of the macromolecular structure in the absence of amino groups. [e] The reaction conducted at 40 °C yielded 94% product after 13 hours.

reaction to explore the catalytic efficiency of chitosan and, as an application case, the synthesis of a drug intermediate synthesis.

A blank control reaction (Table 1, entry 1) between benzaldehyde (**1**, 2 mmol) and ethyl cyanoacetate (**2**, 2.1 mmol) in ethanol at room-temperature delivers only traces of product after 72 h, as confirmed by gas chromatography (GC). The reaction (Table 1, entry 2) using 25 mg chitin as the catalyst (the untreated polysaccharide bearing no amino groups) yielded less than 3% of product after 48 h. In stark contrast the same amount of chitosan gave 45% product yield, and 50 mg of chitosan gave 93% yield after 24 h (Table 1, entries 3 and 4). This comparison clearly confirms that the amino groups are responsible for the high yields, acting as catalyst.

The product yield and purity were confirmed by GC, electrospray ionization high-resolution mass spectrometry (ESI-HRMS), ^{1}H NMR, and ^{13}C-NMR (see SI for details). Room temperature (RT) and ethanol were kept to match sustainable chemistry standards. To investigate the catalytic efficiency and reusability of chitosan, the reaction was repeated six times after filtering and drying pre-used chitosan at 40 °C under reduced pressure for 2 h (Table 1, entries 4–9). All six reaction cycles produced high yields without loss of catalytic activity. Additionally, not only chitosan was recovered and reused after each cycle, but also ethanol, by using a rotary evaporator. The recovered ethanol (2.5 mL) was mixed with additional 0.5 mL from ethanol recovered from washing

chitosan. Also, a total of approximately 2.3 g of product **3** (Scheme 1) was produced by using 50 mg of chitosan as catalyst and using 6 mL of ethanol for six reactions cycles. Additionally, when the reaction was conducted at 40 °C, a 94% yield was achieved in just 13 h however, this came at the cost of a 10% increase in energy consumption due to the elevated temperature (entry 10). Furthermore, increasing the catalyst mass to 100 mg slightly reduced the reaction time to 20 h with a yield of 95% (entry 11). However, such increased catalyst amount required additional solvent to maintain proper dispersion, more solvent for catalyst washing, and longer drying time after the reaction cycle, all of which increased the energy and resource demands. Overall, a total electrical energy of *ca.* 0.2 kWh was determined for a complete reaction cycle in this case, yielding *ca.* 1.9 mmol of products, which varies depending on timing and conditions (*vide infra*).

Notably, quantifying the molar percentage of active amino groups in chitosan particles presents a significant challenge due to their large particle sizes and the presence of potentially inaccessible amino groups. According to the supplier, the chitosan material used in this study is 75% deacetylated, and elemental analysis indicates approximately 0.55 mmol g^{-1} of nitrogen, suggesting an expected content of 0.41 mmol g^{-1} of amino groups. Based on this, 50 mg of chitosan contain 0.0205 mmol of amino groups. However, the actual number of surface-active amino groups is likely much lower. Attempts to confirm this value *via* the Kaiser test proved difficult, as the bulky reagents were probably unable to access the hindered amino groups within the macromolecular network. Similarly, acid–base titration was unsuitable due to chitosan's solubility in acidic media, while for the catalytic reaction chitosan is present as a solid, undissolved particles. As a result, as catalyst quantity we give the mass of chitosan (in mg) rather than an exact molar percentage of amino groups.

The reaction was further subjected to different substrates that resulted in similarly high yields (Scheme 2, **3–13**). In most cases, reactants were fully converted into their condensation products after 24 h. With terephthalaldehyde, the reaction was completed after already 8 h leading to the appearance of the ethanol-insoluble solid product (product **4**, Scheme 2), while 2-naphthaldehyde and 9-anthracenecarboxaldehyde required 30 and 36 h for full conversion to **11** and **13** respectively. Given the nearly complete conversion and high selectivity, the products were characterized after drying at room temperature without further purification (except **13**). The yield and purity of all products was checked by electrospray ionization high-resolution mass spectrometry (ESI-HRMS), ^{1}H NMR, and ^{13}C NMR spectroscopy (all mass and NMR spectra are provided in the SI file). The MS data showed no signals corresponding to side products, while trace impurities were detected that were attributed to common silicon grease contamination from the glassware. On average a yield of 96% was obtained throughout all reactions based on the final weight of solid products. All products exhibited the thermodynamically favoured *E* isomer, as determined by ^{1}H-NMR, except for **13** which shows 93% *E* isomer. The spectra were compared and found to be
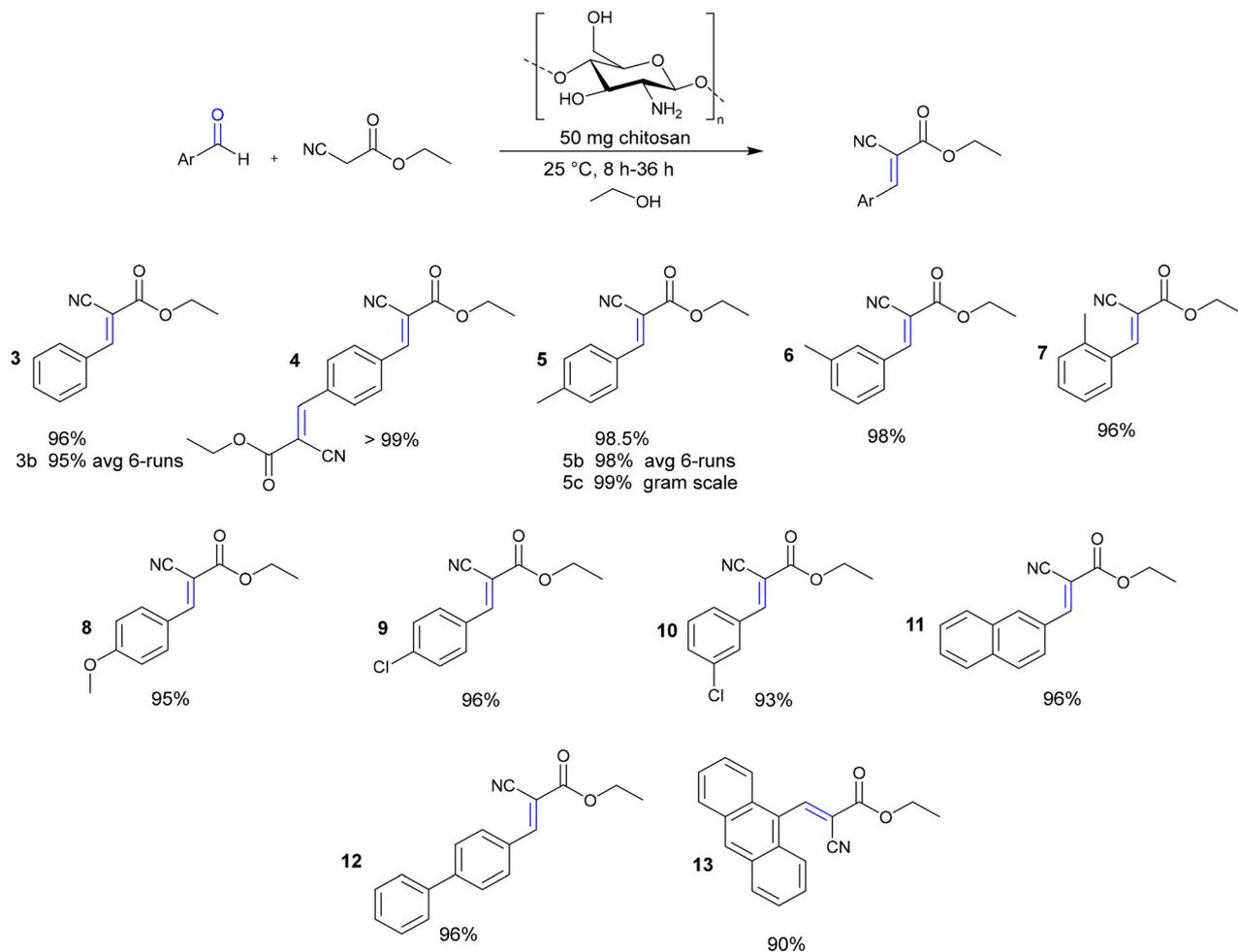
Scheme 2 Substrate scope of substituted benzaldehydes reacting with ethyl cyanoacetate using chitosan as catalyst under optimized conditions[a–d]. [a] 2 mmol benzaldehyde derivative, 2 mmol ethyl cyanoacetate. [b] Ethanol used as solvent for all the reactions except for 13 where a 1 : 2 mixture of ethanol and toluene (in volume) was used because of solubility issues. [c] General reaction time of 24 h except entries 4, 11, and 13 with 8 h, 30 h and 36 h, respectively. All reactions carried out at 25 °C except for 13 which was carried out at 40 °C to increase solubility. For gram-scale synthesis 5c, a reaction time 48 h and 40 °C were used, and 99% of product was achieved. [d] Products 3b and 5b correspond to the reusability tests of products 3 and 5, respectively, where each reaction was repeated six times using the same 50 mg portion of chitosan across all cycles; for entry 5c, 300 mg recycled chitosan was reused for gram-scale synthesis. For product 13, 100 mg of chitosan was used.

consistent with those previously reported in the literature (shown in the SI file). For **5b**, the reaction was run six times by reusing 50 mg chitosan as catalyst, resulting in 98% yield on average, and no loss in catalytic activity was observed. Before reusing in a subsequent run, chitosan was dried at 40 °C under reduced pressure oven for 2 h to evaporate ethanol and traces of water, so that after 2 h another reaction was ready to run (see Fig. 6 for the synthetic process). With the goal to investigate for upscaled synthesis using chitosan as catalyst, a gram-scale synthesis of **5** was carried out (**5c**, Scheme 2) using 300 mg of already used chitosan that yielded 4.30 g (99%) of product after 48 h. This result shows that gram-scale synthesis performs equally well. Overall, the straightforward nature of the process helped to minimise product loss.

To assess the energy demand of the one-pot synthesis, the energy consumption was calculated at every step by using an electricity meter. The total electric energy consumption for the

synthesis was 0.212 kWh encompassing the entire synthesis chain (26.5 h), for the synthesis of *ca.* 2.0 mmol of products. For comparison, this amount of energy is approximately what a typical laptop (≈ 60 W) would consume if operated for about 3.5 h. Overall, stirring for 24 h at room temperature consumed 0.136 kWh, suction filtration took 5 min and 0.022 kWh, the rotary evaporator used 0.048 kWh in 20 min, and drying in a vacuum oven for 2 h required 0.006 kWh. The energy cost may vary based on stirring time and temperature adjustments, of course. Yet, the mild conditions and one-pot synthesis thus made the overall process quite energy-efficient. As chitosan was purchased from suppliers, the energy consumption during conversion of the shrimp's exoskeleton to chitosan is not included in these calculations. However, it is expected not to be high as the process involves chemical extraction of chitosan at a maximum temperature of 100 °C for 3 h.[42] In summary, the total energy consumption of this process is still low on an

Table 2 Comparison of different catalytic systems, for the Knoevenagel condensation between benzaldehyde and ethyl cyanoacetate, with the present study

No#	Catalyst	Temperature (°C)	Time (h)	Yield (%)	Catalyst reusability	Ref.	Price[i]
1	Au(OCH$_2$CF$_3$)(PPh$_3$)	50	97	93	NR	43	400–450 US$ per g
2	Fly ash supported CaO[a]	90	2	83	3	50	300–500 US$ per g
3	Carbon Nitride	Microwaves	0.2	87	5	45	Ca. 1- 10 US$ per g
4	UMCM-1-NH$_2$[b]	40	2.2	73	3	46	500 – 3000 US$ per g
5	AP-SiO2@Fe$_3$O$_4$[c]	RT	1.5	90	5	44	550 US$ per 10 mL g^{-1}
6	Na-A-PW9[d]	RT	6	83	6	47	54–104 US$ per g
7	MCM-41-APTMS[e]	80	4	95	4[f]	48	60–105 US$ per g
8	Silica monolith-APTMS[g]	RT	Flow	87	NR[g]	6	650–1400 US$ per column
9	PgBd-porous organic polymer[h]	60	24	96	6	49	60–125 US$ per g
10	Chitosan	RT	24	96	6	This study	6 US$ per g

[a] Catalyst was reactivated at 700 °C for 2 h before use. [b] UMCM-1-NH2 = University of Michigan crystalline material-1-amine. [c] AP = aminopropyl. [d] Tri-lacunary polyoxometalates of Na$_8$H[A-PW$_9$O$_{34}$]. [e] APTMS= (3-aminopropyl)triethoxysilane. [f] Catalytic activity gradually decreased to 50% at 4th cycle. [g] Flow catalysis by connecting APTMS-silica monolithic column to an HPLC pump, 30% loss in catalytic activity after 65 h of continuous use. [h] PgPb = phloroglucinol and benzidine. [i] Prices are estimated from multiple suppliers (lowest to highest); unavailable prices were approximated for respective precursors of catalysts as of 25 Jun 2025 with help of ChatGPT.

absolute scale, largely owing to the efficiency of the one-pot synthetic approach.

To have a critical and comparative analysis of our work in terms of sustainability, we compared our study to already reported protocols for the synthesis of **3**. Table 2 compares chitosan with different solid heterogeneous basic catalysts used to catalyse the reaction between benzaldehyde and ethyl cyanoacetate, comparing relevant sustainability parameters. Apparently, chitosan stands out as a significantly more cost-effective option, and an environmentally friendly and sustainable choice for this reaction compared to other catalysts. All alternative catalysts are either metal-based[43,44] and/or they are prepared through multistep syntheses partially involving hazardous reagents.[6,43–49] A meaningful comparison of energy consumption is challenging, as the synthesis of these catalytic systems often involves multiple steps, the energy consumption of which not being reported, including the functionalization of organic catalysts onto support materials in some cases (Table 2 entries 4 to 8). The yields are significantly lower for these catalysts, and the reusability is substandard as compared to chitosan. Some of these catalysts gradually degrade upon continuous re-use,[6,46,48] and some of them require higher temperatures for reactivation.[50] Thus, a comparison of these ten catalysts already indicates good compatibility of chitosan as catalyst with certain principles of sustainable chemistry, which is scrutinised below (Table 4).

As solid chitosan showcased remarkable efficiency as basic catalyst for the Knoevenagel condensation and high reusability, we studied its use in the synthesis of an industrially produced drug, namely an intermediate in the synthesis of Atorvastatin.[39]

Pfizer's Atorvastatin synthesis route is summarized in Scheme 4.[39] Intermediates **19** and **20** (highlighted in blue boxes) are synthesised separately and then undergo a reaction to the target molecule Atorvastatin **22** after two additional steps. Most Atorvastatin-related syntheses focus on intermediate **20**. For the synthesis of intermediate **18**, 4-methyl-3-oxo-N-phenyl-2-(phenylmethylene)pentanamide (highlighted in the green box, Scheme 4) only a handful of studies are available (Table 3). In contrast, most reported synthetic routes toward

Table 3 Comparison of already reported synthetic conditions for Atorvastatin intermediate **18** with the conditions used in the present study

No#	Catalyst	Temperature °C	Time (h)	Yield %	Ref.
1	Piperidine/AcOH	84	3	80	40
2	β-alanine/AcOH	61	21	NR	53
3	4-Aminophenole/AcOH	69	24	93	55
4	MNPs-IT-PA	80	4	84	54
5	DABCO-PDO/AcOH	RT	3	83	56
6	DMAP/HCOOH	120	Flow	36	57
7	Chitosan	RT	26	> 96	This study

Atorvastatin start either from **18** or, in most cases, from intermediate **19**.[40,51–54] Frequently, new reported total synthetic approaches rely on a previously established route for the synthesis of **18** where β-alanine and acetic acid are used as catalysts applying an energy intensive Dean–Stark trap step.[53] Here, we present a facile and sustainable synthesis for **18**, performed at room temperature, utilizing chitosan as the catalyst in acetone, without additives, resulting in an excellent yield of 96% after 26 h (Scheme 3). The synthetic process is described in detail in the "Experimental section".

The high yield was confirmed by ESI-HRMS, ^{1}H-NMR and ^{13}C-NMR spectroscopy (spectra given in the SI file). Although the ^{1}H-NMR spectrum shows an *E* and *Z* isomer mixture, this is irrelevant for the subsequent step of **19** as it involves the addition of *para*-fluorobenzaldehyde to the double bond of **18** to form racemic **19**. By utilization of solid chitosan as a catalyst, along with acetone as solvent at room temperature, this synthesis stands out as sustainable and cost-effective. As two equivalents of benzaldehyde were used for the synthesis of **18**, removal of excess benzaldehyde was accomplished by a silica column using hexane and ethyl acetate 30 : 1. Evidently, the use of hexane is undesired, but was inevitable for purification. Future work might find less harmful procedures for this step.

Table 3 provides a comparison of well-known reported syntheses for **18** with the approach presented in this study. Our method not only achieves higher yields but also stands out
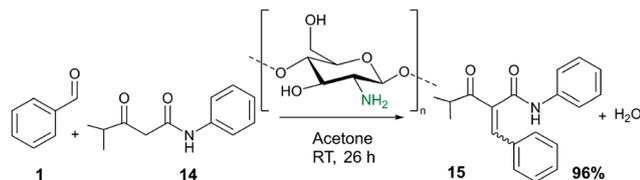
Scheme 3 Synthesis of 4-methyl-3-oxo-N-phenyl-2-(phenylmethylene)pentanamide using solid chitosan as catalyst in acetone at room temperature.

due to a one-pot synthetic approach without additives (*e.g.*, absence of acid), room-temperature conditions, and the ability to reuse the catalyst. Contrarily, entries 1 to 6 in Table 3 lack catalyst reusability, except for entry 4 where a heterogeneous catalyst (propylamine modified with imidazolium ions on magnetic nanoparticles) can be reused multiple times. Entry 6 represents a recent study using a continuous-flow approach. However, the homogeneous catalyst DMAP poses potential hazards owing to toxicity. Overall, the use of unsustainable solvents and catalysts, and high-temperature conditions in all reported methods renders them incompatible with several principles a "green"/sustainable chemistry.

Furthermore, using chitosan as a catalyst offers the distinct advantage of avoiding a procedure to remove water in the synthesis of **18**. The effectiveness of chitosan in this context arises from its peculiar macromolecular structure, which is rich in amino and hydroxyl groups. These groups result in a marked binding capacities and swelling capacity ($S_\%$) in protic solvents.[58] Cho *et al.* reported WBC values ranging from 458% to 805% for chitosan, extracted from shrimp shells; the values depend on the degree of deacetylation (DD) and bulk density.[59] In our study, the WBC of chitosan was determined using the method developed by Wang and Kinsella.[60] The chitosan material employed as catalyst was 75% deacetylated and exhibited a WBC value of 520%. This value is 29-fold higher than the amount of water (1 mmol or 18 mg) released during

the condensation reaction for synthesizing **18** with our standard procedure (using 213 mg benzaldehyde). Additionally, the ethanol-binding capacity (EBC), measured using the same method, was found to be 104%. These high binding capacities for protic solvents facilitate the rearrangement of chitosan's polymer chains, presumably exposing more catalytic sites, which can be further understood through a swelling experiment, providing the percentage of solvent kept after the swelling experiment ($S_\%$). The $S_\%$ values were determined using the method developed by Gupta *et al.*[61] resulting in values of 607% for chitosan in water and 171% in ethanol. These results highlight a crucial property of chitosan in protic solvents—its ability to swell, thereby increasing the surface area and exposing more catalytic sites, ultimately enhancing its catalytic efficiency. Fig. 2 illustrates the swelling of chitosan in a polar solvent, making hindered catalytic sites (amino groups) available for reactants in polar solvents. In our study, vigorous stirring probably further promoted the swelling in ethanol. Furthermore, the high WBC efficiently removes water from the reaction. This dual functionality, namely acting as both a catalyst and an efficient water-binding agent, can explain the high yields in repeated runs. These features represent a distinct property of chitosan, simplifies the reaction setup and process, and thereby provides a sustainable alternative to traditional methods.

To further investigate water–vapour interaction at the molecular and structural levels, water vapour sorption of chitosan and chitin was measured at two different temperatures (Fig. 3). The water vapour sorption isotherms for chitosan (blue curves in Fig. 3A) indicate pronounced water vapour uptake values of 493 cm^3 g^{-1} and 436 cm^3 g^{-1} at 25 °C and 80 °C, respectively, compared to chitin (black curves), which shows water uptake values of 237 cm^3 g^{-1} and 269 cm^3 g^{-1} at the maximum achievable relative pressure ($p/p_0 = 0.97$).

As relative humidity increases, the volume adsorbed by both chitosan and chitin rises, reaching maximum levels at full saturation. To illustrate the magnitude of the water vapour
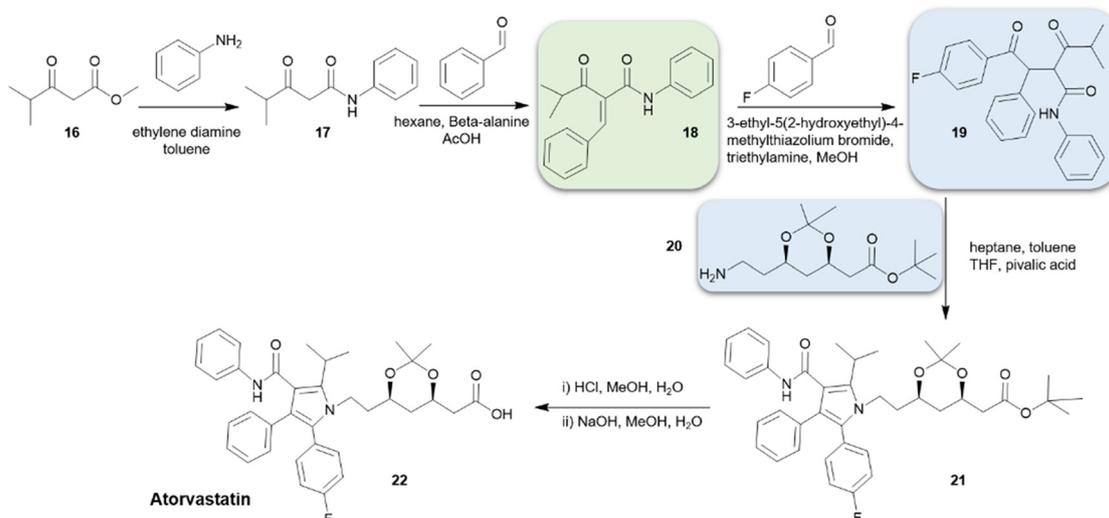
Scheme 4 Synthesis of Atorvastatin followed by Pfizer at the commercial level.
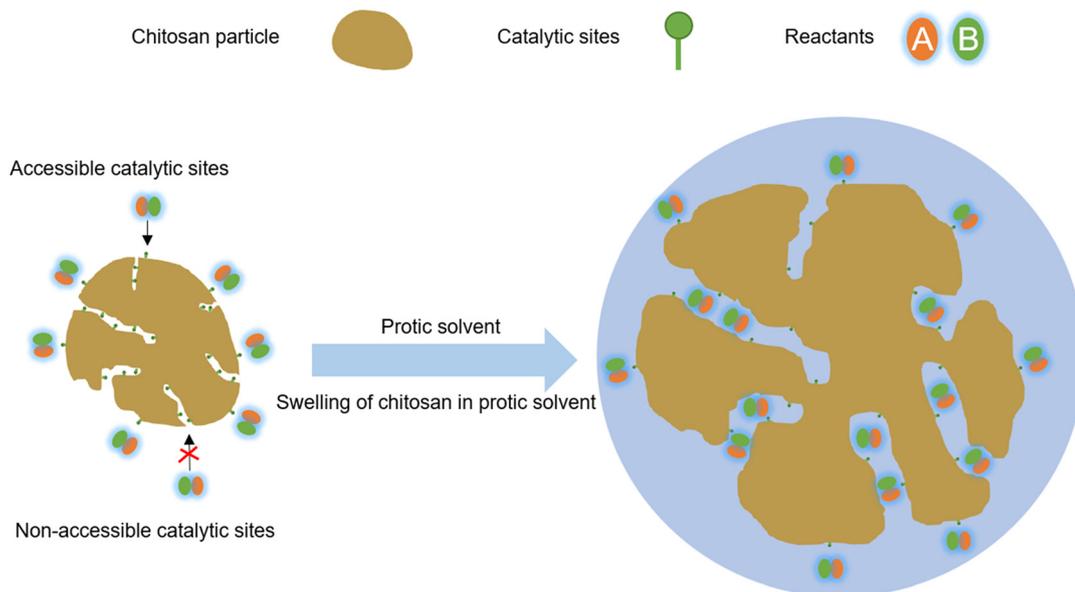
Swelling of chitosan in protic solvents like ethanol due to interactions with hydroxyl and amine groups enhances exposure of catalytic sites for reaction, while its hydrophilicity aids in water capture, facilitating reactions requiring water removal.

Fig. 2 Swelling of chitosan in protic solvents due to interaction with hydroxyl and amino groups of chitosan.
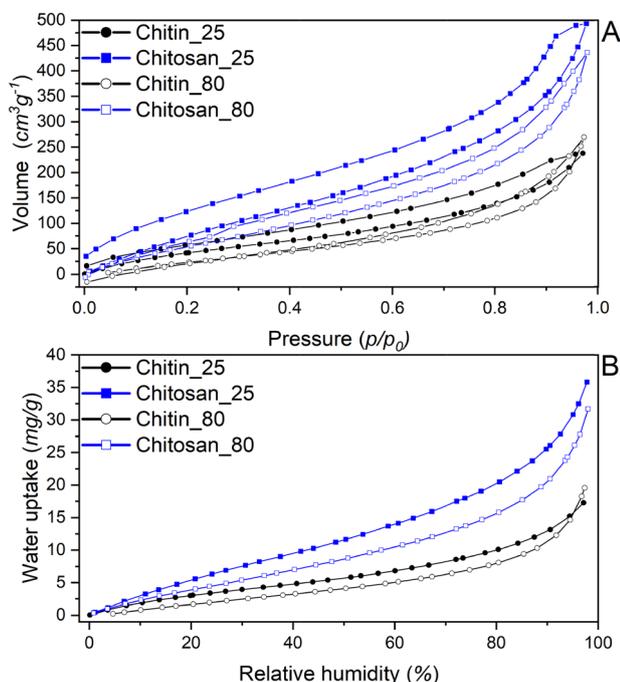

Fig. 3 Water vapour sorption analysis of chitin and chitosan at 25 and 80 °C, (A) Water vapour sorption isotherms showing adsorb volume of vapours per gram of chitosan at maximum p/p_0 = 0.97. (B) amount of water vapour sorption in milligram as function of relative humidity.

whereas chitin adsorbs only 17 and 19 mg g^{-1}. The higher adsorption capability of chitosan is attributed to its amine and –OH groups, and a significantly larger BET surface area is estimated from water sorption (150 m^2 g^{-1} for chitosan compared to 50 m^2 g^{-1} for chitin). Notably, in protic media or under high humidity, chitosan undergoes structural rearrangement due to an acid–base reaction, its strong solvent-binding capacity, and swelling behaviour. As a result, its effective surface area varies significantly depending on the environmental conditions—whether in dry powder form, in water, or in ethanol.

The temperature-dependent differences in the adsorption behaviour give further insight into the water uptake: as seen in Fig. 3 the chitosan water vapour uptake is smaller for the higher temperatures (80 °C) at all pressures. This marked difference is due to the strongly exothermic interaction of water with amino and hydroxy groups. The water vapour isotherms even allow for estimating the isosteric adsorption enthalpy ΔH_{ads}. In essence, ΔH_{ads} can be evaluated from the data shown in Fig. 3 A by using the pressures measured for different temperatures, for the same coverage ϑ, in the range of surface binding. For the two available temperatures we used the two-point approximation

$$\left\{\frac{\Delta \ln (p)}{\Delta \left(\frac{1}{T}\right)}\right\}_{\vartheta} = \frac{\Delta H_{ads}}{R}$$

Taking several volumes in the low-pressure range, corresponding to the adsorption of water molecules to the chitosan surface, rather than to condensation of water, we obtain ΔH_{ads} values of *ca.* 10 kJ mol^{-1}. Such values are in sound agreement with the typical values for hydrogen bonds, *i.e.*, can be interpreted as the interaction of water molecules with amino and

uptake, these sorption isotherms were converted into a more comprehensive form (Fig. 3B), *i.e.*, by calculating the relative increase in mass *vs.* relative humidity. This representation reveals that at maximum relative humidity, chitosan adsorbs 36 and 31 mg g^{-1} of water vapour at 25 and 80 °C, respectively,

hydroxy groups of chitosan. Hence, the data confirm strong binding of water to chitosan, which further supports the view that water as reaction product is removed from the reaction mixture, thus leading to high yields. In summary, chitosan exhibits superior water uptake compared to chitin, driven by molecular and structural differences that enhance its interaction with water vapour.

Stability of solid chitosan as catalyst

Chitosan exhibited high stability with respect to the catalytic action after being used repeatedly as a catalyst and being subsequently recovered. To analyse physical and chemical changes, chitosan was characterized using various techniques for comparisons after multiple reaction cycles. Fig. 4 shows SEM images of chitosan prior to and after six-fold use as catalyst. At first glance, no structural changes between fresh (Fig. 4A) and used chitosan (Fig. 4C) are visible. Higher magnification reveals some structural alteration, in that the initially smooth surface (Fig. 4B) is not preserved but appears patchy after multiple use (Fig. 4D). However, these scratches could just be a result of vigorous stirring during the reaction which apparently does not affect the catalytic performance.

Fig. 5A shows a mercury intrusion porosimetry (MIP) analysis that was carried out to analyse structural changes possibly leading to creation or closure of meso/macropores after using chitosan as catalyst, *e.g.*, introduced by vigorous stirring. Essentially, MIP data show no significant difference in the porosity in pristine and used chitosan. The population of large macropores is assigned to interparticle voids which slightly change after the reaction, probably because of stirring. The absence of nanopores in MIP seems to be at variance with the marked nanoporosity detected in water sorption, yet the latter is based on strong chemical interaction and swelling.

Diffuse reflectance infrared Fourier transform spectroscopy (DRIFT) analysis of chitosan before and after catalysis (Fig. 5B) does not indicate any changes of the organic functionalities.
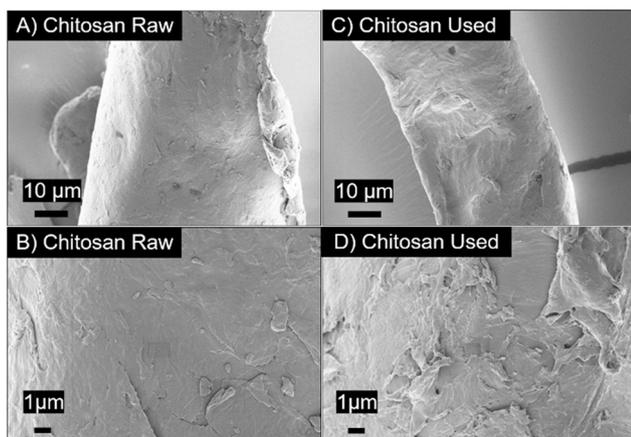

Fig. 5 (A) Mercury intrusion porosimetry data show the emergence of a small mesopore volume after six-fold use of chitosan that are possible slits created by intensive stirring of chitosan while the population of macropores is due to interparticle voids, (B) DRIFT spectrum of pristine chitosan and after six-fold use showing no differences, (C) the XRD analysis of pristine and used chitosan showing no significant difference in the crystallinity, which is seen be the prominent signal at $2\theta = 20°$. The change at smaller diffraction angles might be due a part of the chains being rearrangement.

To further investigate possible changes on the atomic level, both pristine and used chitosan were subjected to powder XRD analysis (Fig. 5C), exhibiting two prominent signals at *ca.* $2\theta = 10$ and $20°$. These broad signals are characteristic of chitosan, highlighting its amorphous nature.[26] However, formally using the Bragg equation, the signals correspond to a repeating dimension of 0.9 nm and 0.4 nm, respectively, which can be qualitatively attributed to the average distance of the polysaccharide chains. After six reaction cycles, the signal at $2\theta = 10°$ disappears, and a signal at $2\theta = 6°$ is observed, likely due to the rearrangement of polymer chains during chitosan swelling in ethanol under rigorous stirring or by repeated heat treatment during drying after each reaction cycle. Yet, the signal at $2\theta = 20°$, being attributable to the arrangement of chains themselves, is unchanged, confirming the structural integrity of the material on the atomic level.

Fig. 4 SEM images of chitosan (A) & (B) before and after six time use as a catalyst (C) & (D) shows that the surface of chitosan is not changed as chitosan is quite stable in organic solvents. Only image (D) shows that the surface of chitosan is scratched due to aggressive stirring during the course of reaction.
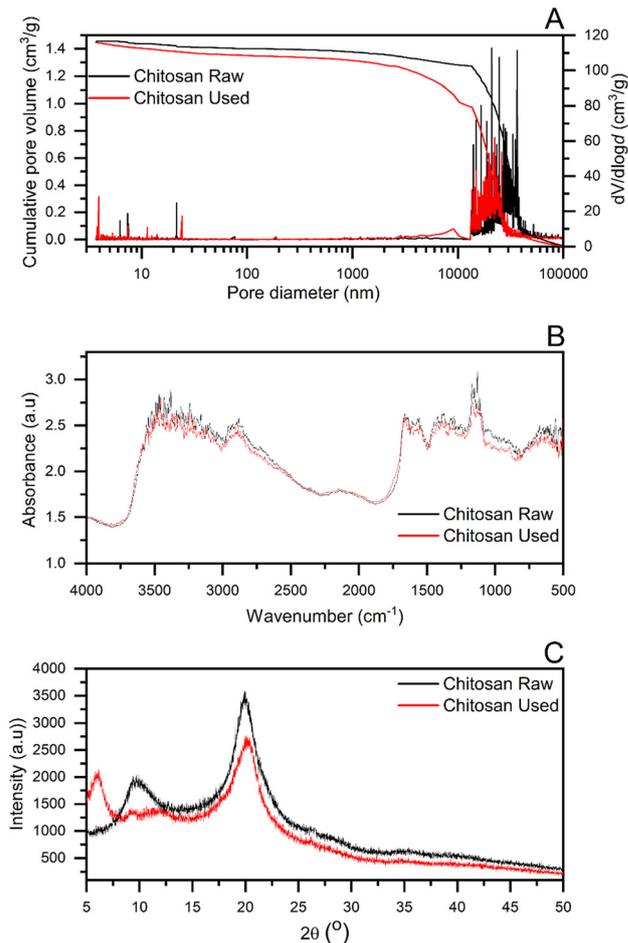
Table 4 Comparison of the present study with the 12 principles of green chemistry

#	"12 Principles of green chemistry"	Present work alignment with principles of green chemistry	Sustainability parameters
1	Waste prevention	Focus on recovery and reuse of catalyst and solvents to reduce waste.	Six reuses of catalyst, Six reuses of ethanol
2	Atom economy	Only water is eliminated, >95% average yield.	Atom economy = 93% Effective atom economy = 89%
3	Less hazardous chemicals synthesis	Simple one-pot synthesis, mostly pure products, eco-compatible solvents.	Chitosan = biopolymer, nontoxic, edible Ethanol, acetone = Eco-friendly solvent Ethyl acetate = problematic Hexane = hazardous
4	Designing efficient but safer products	Eco-friendly solvents, biodegradable, and efficient catalysts, and energy-efficient, one-pot synthesis of condensation products.	Sustainable method, efficient catalyst, and safe.
5	Eco-friendly solvents and reagents	Exclusive use of eco-friendly ethanol and acetone for reaction solution, biopolymer chitosan as catalyst.	Chitosan = biodegradable Ethanol, acetone = eco-friendly solvents Ethyl acetate = problematic Hexane = hazardous
6	Design for energy efficiency	Room temperature for all reactions, 40 °C for only one entry.	0.348 kWh utilised for synthesis of 4.3 g of product (**3c**, Table 5)
7	Use of renewable feedstock	Source of chitosan is the shrimp exoskeleton (chitin), which is otherwise wasted	Chitosan source = shrimp exoskeleton
8	Reduce derivatives	Highly selective reactions, mostly no purification. Only solvent evaporation to collect pure product.	Overall chemoselectivity => 96%
9	Catalyst	Green catalyst with high selectivity, efficiency, and reusability	Overall chemo-selectivity => 96% Reusability = six reaction cycles, no loss in activity
10	Design for degradation	Chitosan, ethanol, and acetone are biodegradable and nontoxic.	Process = reusable apparatus and auxiliaries, catalyst and solvents biodegradable
11	Real-time analysis for pollution prevention	During product formation, no gases released, only water is eliminated, solvents were reused.	Acetone evaporated during separation of products on rotary evaporator
12	Safer chemistry and processes	One-pot synthesis, only stirring required, mostly no purification step needed.	Major steps = stirring, evaporation of solvent from products, washing of chitosan to reuse.

Comparative analysis of present study to the principles of green chemistry

To evaluate the overall sustainability systematically, we relate the present work to the twelve principles of green chemistry stated by Anastas and Warner in 1998.[62] Table 4 shows a comparative analysis of the present study with these principles of green chemistry and calculated green factor values.

Conclusions

We demonstrate high catalytic performance and sustainability of chitosan in the Knoevenagel condensation between benzaldehyde derivatives and ethyl cyanoacetate. Chitosan gave high yields (90–99%) across various substrates. Optimising the catalyst amount to 50 mg for *ca.* 212 mg of benzaldehyde resulted in an average yield exceeding 95%, as confirmed by GC, ESI-HRMS, ^{1}H-NMR and ^{13}C-NMR spectroscopy. The catalyst exhibited excellent reusability, maintaining its catalytic efficiency over six reaction cycles with yields consistently between 95% and 98% for different substrates. Additionally, the recovery and reuse of the solvent ethanol, further highlights the sustainable features of this process. The one-pot synthesis approach renders the synthetic process simple and straightforward.

Broadening the scope of chitosan's application for the synthesis of important drug intermediates, we demonstrated its efficacy as catalyst in the one-pot synthesis of an Atorvastatin intermediate, 4-methyl-3-oxo-*N*-phenyl-2-(phenylmethylene)

pentanamide, achieving a yield of 96% at room temperature. Note that the reaction mixture contains only the reactants, solvent, and chitosan, *i.e.*, making the process particularly promising in terms of separating products, solvents and catalyst without the need for elaborate processes. This method outperforms other reported approaches in terms of yield, simplicity, and environmental impact. The gram-scale synthesis of the Atorvastatin intermediate further confirmed the viability of chitosan as a catalyst for the sustainable synthesis of other fine chemicals.

The high water and ethanol-binding capacities of chitosan (WBC = 520%, EBC = 104%) highlight its dynamic structural behaviour in protic solvents and is one of the reasons for the high yields. On one hand, its high-water uptake ability captures water released during the reaction, thus shifting the composition towards the product side. On the other hand, its significant sponge-like swelling in ethanol (171%) enhances the accessibility of catalytic sites, further boosting performance. This dual functionality underscores chitosan's adaptability and effectiveness as a catalyst in water-releasing reactions. Yet, our studies on the solvent uptake also show the need for in-depth studies on the state of water and solvent insight the chitosan gel, and also to which extent a chitosan particle is infiltrated by the solvent. SEM, MIP, DRIFT, and XRD analyses validated the chemical and morphological stability of chitosan, showing no significant degradation after multiple uses, thus ensuring its potential for recyclable application. Our method performs promisingly compared to reported approaches in terms of yield, simplicity, costs and environmental impact, suggesting

chitosan's potential in pharmaceutical syntheses. Moreover, the reactions featured nearly complete conversion ($\sim$100%) and high selectivity ($\sim$96%). ESI-HRMS revealed the absence of impurities for most of the synthesized compounds. Thus, the products were characterized without further purification, although additional purification may be applied for pharmaceutical applications where removal of trace impurities is critical.

In comparison to catalysts from 15 other studies, chitosan provided competitive or superior yields and sustainability. Many conventional catalysts demonstrated lower reusability and higher environmental impact, whereas chitosan's biodegradable and non-toxic nature aligns well with "green chemistry" principles, rendering it a promising alternative. Note that the high yields achieved in our study are certainly partially due to the relatively high amount of catalyst used, in relation to the reactants. These high yields are indeed due to the catalytic action of the amino groups and not only by the high WBC, as chitin exhibits low yields, whilst possessing a high WBC, too. However, because of the abundance, facile separation, and reusability of chitosan here the amount and costs of the catalyst are not critical factors. Thus, the chitosan-catalysed process aligns well with several principles of sustainability: high yields, eco-friendly solvents (ethanol and acetone), energy efficiency (room-temperature reactions), and minimal waste generation.

Based on our findings, we propose that chitosan points to an attractive general concept in organocatalysis: using a solid abundant, non-toxic catalyst material, containing a large number of catalytic motifs, and at the same binding to – thereby deactivating – a condensation by-product might be applicable in the synthesis of other relevant fine chemicals.

Future research should therefore focus on exploring chitosan's catalytic potential in other synthetic processes, including base catalysis or by modifying the surface to obtain a different catalytic motif.

Experimental section

Chemical and materials

Chitosan was purchased from Sigma-Aldrich with a reported degree of 75% deacetylation, starting from Chitin (exoskeleton of shrimp as source), Chitin (Sigma-Aldrich, exoskeleton of shrimp as source), ethyl cyanoacetate (Sigma-Aldrich >98%), benzaldehyde (Sigma-Aldrich >99%), *p*-tolualdehyde (Sigma-Aldrich 99%), *m*-tolualdehyde (BLD Pharma 99.72%), *o*-tolualdehyde (BLD Pharma 99%), *p*-anisaldehyde (TCI > 99%), 4-chlorobenzaldehyde (Sigma-Aldrich 97%), 3-chlorobenzaldehyde (TCI 98%), terephthalaldehyde (TCI >98%), 2-naphthaldehyde (Fisher Scientific 98%), 4-biphenylcarboxaldehyde (Fisher Scientific 99%), 9-anthracenecarboxaldehyde (Sigma-Aldrich 97%), 4-methyl-3-oxo-*N*-phenylpentanamide (BLD Pharma 99.5%), absolute ethanol (Fisher Scientific 99.8%), hexane (Sigma-Aldrich, HPLC grade), ethyl acetate (Sigma-Aldrich, HPLC grade), toluene (thermo scientific 99.85%)

and acetone (Sigma-Aldrich 99.5%). All the chemicals were used without further purification.

Methods for analysis

Mass spectrometry (MS). Mass spectrometry was performed by using Bruker Impact II (ESI-HRMS) by using methanol as the carrier.

Nuclear magnetic resonance spectroscopy (NMR). ^{1}H NMR and ^{13}C NMR spectra were measured with a 400 MHz spectrometer (Bruker Avance III HD, Bruker BioSpin GmbH, Rheinstetten, Germany) at 25 °C. CDCl$_3$ and DMSO-d_6 were used as solvent.

Water and ethanol-binding capacity. WBC of chitosan was assessed by placing 0.5 g of chitosan sample into a pre-weighed centrifuge tube. Next, 10 mL of distilled water was added, and the sample was mixed using a vortex for 1 min to ensure proper dispersion. The mixture was allowed to rest at room temperature for 30 min, with alternating shaking for 5 s every 10 min. Following this, the sample was centrifuged at 3200 rpm for 25 min. After carefully removing the supernatant, the tubes were weighed again. The WBC (%) was determined using the following eqn (1). The same method was used to measure the ethanol-binding capacity of chitosan.

$$\text{WBC}\,(\%) = \frac{(\text{Water bound (g)})}{(\text{Initial sample weight (g)})} \times 100 \quad (1)$$

Swelling. To determine the swelling properties, 0.5 g of dry chitosan was immersed in 15 mL of either deionized water or absolute ethanol. The samples were allowed to swell for 24 h at room temperature. After swelling, chitosan was removed, excess liquid was drained, and the swollen sample was weighed. The swelling percentage was calculated using the eqn (2),

$$S_\% = \frac{W_s - W_d}{W_d} \times 100 \quad (2)$$

where W_s is the mass of swollen chitosan, W_d is the mass of dry chitosan.

Water vapour sorption analysis. Water vapour sorption analysis was performed by using a vapour sorption volumetric gas sorption analyser VSTAR (Quantachrom). The samples were degassed at 80 °C for 12 h before analysis. Two temperatures (25 °C and 80 °C) were used for comparative analysis of chitin and chitosan.

Scanning electron microscopy (SEM). Smart SEM MERLIN (Carl Zeiss) scanning electron microscope was used for scanning electron microscopy with acceleration voltage of 1 kV. Chitosan was sputtered with platinum for 60 s before analysis to increase conductivity of the samples.

Mercury intrusion porosimetry (MIP). For porosity analysis a mercury porosimeter Pascal 140/440 (Thermo Fisher Scientific, Rodano, Italy) with a pressure range of 0–400 MPA was used. Washburn equation was applied to analyse the data, using the instrument's software (Sol.I.D). A surface tension of 0.48 N m^{-1} and contact angle 140° were assumed for intruded mercury.

Diffuse reflectance infrared Fourier transform spectroscopy (DRIFT). IR spectra of chitosan were measured using a DRIFT instrument (Alpha II, Bruker Optik, Ettlingen Germany). Dried samples were analysed with a resolution of 4 cm^{-1} and using 80 scans.

XRD. X-ray diffractometry of chitosan samples was measured on an XRDynamic 500 diffractometer by Anton Paar in a 2 Theta range of 5–50°.

One pot synthesis of Knoevenagel condensation products. The method employed for synthesis of the chitosan-catalysed Knoevenagel condensation products from benzaldehydes and ethyl cyanoacetate was simple and straightforward. The one-pot synthesis of all products was carried out without using extreme conditions and complex purification steps. A practical view of the synthetic process can be seen in Fig. 6. A 5 mL one-neck round-bottom flask was utilised for the synthesis of all the products, except for the gram-scale product, where a 25 mL round-bottom flask was used. A 1 cm long magnetic stirrer was used for stirring at 800 rpm, in a flask sealed with a glass plug wrapped in paraffin film. Ethanol was used as the primary solvent for the majority of the products, while toluene was additionally added for the better solubility of 9-anthracene-carboxaldehyde (Table 5, entry 11). The synthesis was mainly conducted at 25 °C, with a maximum temperature of 40 °C selectively used for better solubility of 9-anthracenecarbox-aldehyde (Table 5, entry 11). Reactions were monitored by thin-layer chromatography (TLC). In most cases, after 24 h reactants were fully converted into products. For terephthalaldehyde (Table 5, entry 2) a solid product appeared after 8 h, while entry 10 and 11 took 30 and 36 h, respectively, for full conversion. After reaction completion, chitosan was separated by suction filtration, while ethanol and acetone (5 mL, 1 : 1) were used to wash solid chitosan. The separated dissolved products were then transferred to a rotary evaporator, and solvents were evaporated at 40 °C while the pressure was gradually reduced to 10 mbar. The solid products were collected after solvent evaporation. The products were then characterized *via* ESI-HRMS, and NMR. The used chitosan was dried at 40 °C for two h under reduced pressure and reused for the next reaction. For product **3** and **5**, ethanol from both the reaction mixture and the washing of chitosan was recovered by rotary evaporation, condensed in the collecting flask, and subsequently reused in the same reactions. In contrast, acetone used for washing chitosan was completely evaporated during the product separation step under reduced pressure due to its low boiling point. No purification steps were used for the products except for the product of 9-anthracenecarboxaldehyde (Table 5, entry 11). This product was isolated after running the product through a short silica column using hexane and ethyl acetate (30 : 1) as the mobile phase. After collecting the dissolved product, the solvents were evaporated at 40 °C with gradually decreasing pressure to 10 mbar.

For gram-scale synthesis of entry **3c** in Table 5, 20 mmol of *p*-tolualdehyde and 20 mmol of ethyl cyanoacetate were added
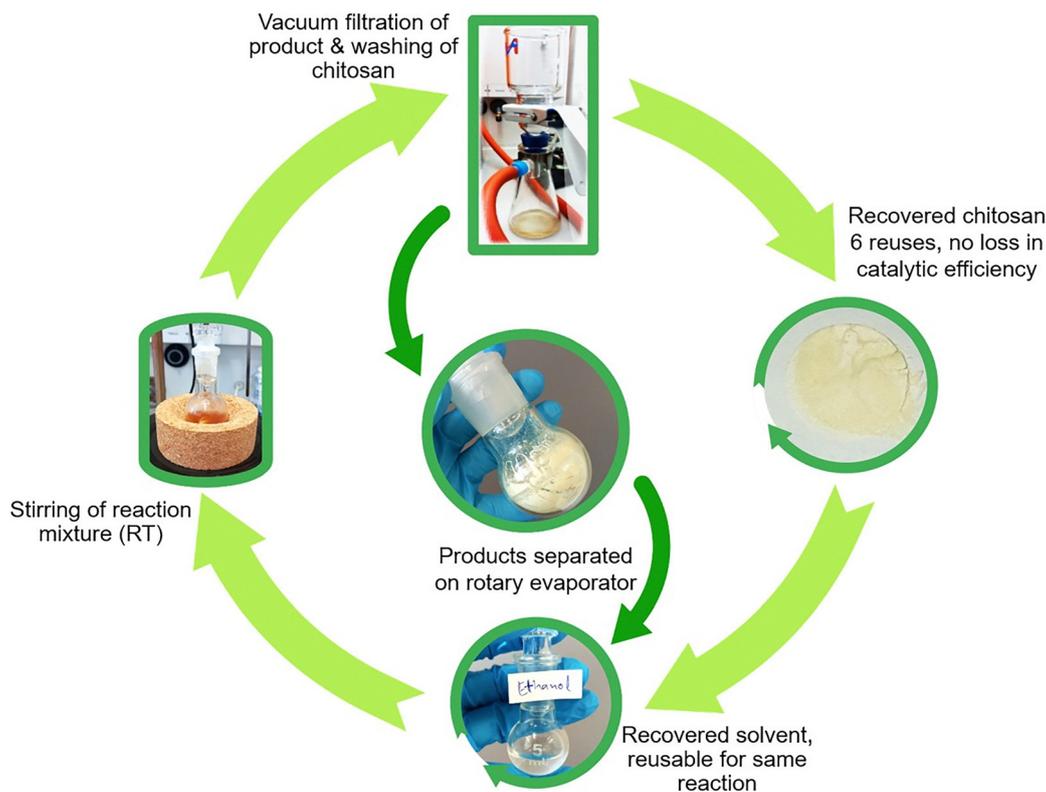

Fig. 6   Practical view for one pot synthesis of Knoevenagel condensation products using chitosan as heterogeneous catalyst.

Table 5 Reaction parameters for the Knoevenagel condensation of benzaldehydes with ethyl cyanoacetate

Entry	Substrates	Scale/mmol	Solvent	Time	Temperature	Chitosan	Yield (%)
1	Benzaldehyde	2 mmol	Ethanol 2.5 mL	24 h	RT	50 mg	96
1b	Six repetitions of reaction	2 mmol	six reuses	24 h	RT	50 mg (reused)	95
2	Terephthalaldehyde	2 mmol	Ethanol 2.5 mL	8 h	RT	50 mg	>99
3	p-Tolualdehyde	2 mmol	Ethanol 2.5 mL	24 h	RT	50 mg	98.5
3b	Six repetitions of reaction	2 mmol	six reuses	24 h	RT	Six reuses	98
3c	Gram-scaled	20 mmol	Ethanol 12 mL	48 h	40 °C	300 mg (recovered)	99
4	m-Tolualdehyde	2 mmol	Ethanol 2.5 mL	24 h	RT	50 mg	98
5	o-Tolualdehyde	2 mmol	Ethanol 2.5 mL	24 h	RT	50 mg	96
6	p-Anisaldehyde	2 mmol	Ethanol 2.5 mL	24 h	RT	50 mg	95
7	4-Chlorobenzaldehyde	2 mmol	Ethanol 2.5 mL	24 h	RT	50 mg	96
8	3-Chlorobenzaldehyde	2 mmol	Ethanol 2.5 mL	24 h	RT	50 mg	93
9	4-Biphenoxycarboxaldehyde	2 mmol	Ethanol 2.5 mL	24 h	RT	50 mg	96
10	2-Naphthaldehyde	2 mmol	Ethanol 2.5 mL	30 h	RT	50 mg	96
11	9-Anthracenecarboxaldehyde	2 mmol	Ethanol/Toluene 1:2, 6 mL	36 h	40 °C	100 mg	90

into 12 mL of ethanol taken in a 25 mL round-bottom flask. 300 mg of recovered chitosan from different reactions was added as catalyst, and the reaction mixture was stirred at 800 rpm and 40 °C. After 48 h, chitosan and product were separated by the same protocol used for other products, and 4.3 g (quantitative yield) of cream-white solid product was collected.

All the reaction conditions and parameters for synthesis of all the products are shown in Table 5. The conditions were selected to achieve sustainability to maximum extent throughout the synthesis processes.

Synthesis of 4-methyl-3-oxo-N-phenyl-2-(phenylmethylene)-pentanamide. For the synthesis of the Atorvastatin intermediate [4-methyl-3-oxo-N-phenyl-2-(phenylmethylene)pentanamide], 100 mg of dry chitosan particles were placed in a 5 mL round-bottom flask. Subsequently, 3 mL of dried acetone, 1 mmol (206 mg) of 4-methyl-3-oxo-N-phenylpentanamide, and 1.5 mmol (213 mg) of benzaldehyde were added, and the mixture was stirred at room temperature. The reaction was monitored by TLC, and after 26 h, chitosan was separated by suction filtration. The crude product was collected by evaporating the solvent using a rotary evaporator. Due to the high boiling point of benzaldehyde, an additional purification step was necessary. Therefore, column chromatography was used to separate the product from benzaldehyde. Thus, benzaldehyde was first isolated from the main product by adding hexane and ethyl acetate (30:1), and then pure ethyl acetate was added in column to collect the purified product. An off-white solid was collected after evaporating the solvents at 50 °C and 20 mbar pressure using a rotary evaporator.

For the gram-scale synthesis of the Atorvastatin intermediate [4-methyl-3-oxo-N-phenyl-2-(phenylmethylene) pentanamide], 400 mg of recovered chitosan was placed in a 50 mL round bottom flask. Then, 15 mmol (3.09 g) of 4-methyl-3-oxo-N-phenylpentanamide and 1.5 equivalents of benzaldehyde (22.5 mmol, 2.27 mL or 2.4 g) were dissolved in 15 mL of dried acetone and stirred at room temperature. The reaction progress was monitored with TLC. Upon completion of the reaction in 48 h, chitosan was separated by filtration under reduced pressure. The dissolved residue was transferred to a rotary evaporator, where acetone was evaporated at 40 °C under a pressure of 10 mbar. After evaporating the acetone, a dense

dark brown liquid was collected and purified using silica column to remove benzaldehyde. Initially, hexane and ethyl acetate (30:1) were used to remove benzaldehyde, followed by the collection of the product using pure ethyl acetate. The solvent was removed by rotary evaporation at 50 °C and 20 mbar pressure. The product was then further dried in a vacuum oven at 40 °C overnight. A total of 4.2 g of off-white solid product was obtained, yielding above 95%.

Author contributions

Conflicts of interest

There are no conflicts to declare.

Data availability

The data supporting this article are available upon request.

Supplementary information: For mass spectrometry, ^{1}H NMR and ^{13}C-NMR data. See DOI: https://doi.org/10.1039/d5nj02915e.

Acknowledgements

goes to the Center for Materials Research (ZfM) at Justus Liebig University Giessen for the support of this project.

References

1 Y. Musa and I. B. Bwatanglang, *Sustainable Nanocellulose and Nanohydrogels from Natural Sources*, Elsevier, 2020, pp. 131–154.

2 C. P. Jiménez-Gómez and J. A. Cecilia, *Molecules*, 2020, **25**, 3981.

3 S. Kamel and T. A. Khattab, *Cellulose*, 2021, **28**, 4545–4574.

4 K. Basavaraju, S. Sharma, A. K. Singh, D. J. Im and D. P. Kim, *ChemSusChem*, 2014, **7**, 1864–1869.

5 W. Zhang and B. W. Cue, *Green techniques for organic synthesis and medicinal chemistry*, John Wiley & Sons, Oxford, 2018.

6 K. Turke, R. Meinusch, P. Cop, E. Prates da Costa, R. D. Brand, A. Henss, P. R. Schreiner and B. M. Smarsly, *ACS Omega*, 2020, **6**, 425–437.

7 J. S. Schulze, R. D. Brand, J. G. Hering, L. M. Riegger, P. R. Schreiner and B. M. Smarsly, *ChemCatChem*, 2022, **14**, e202101845.

8 J. S. Schulze, J. Migenda, M. Becker, S. M. Schuler, R. C. Wende, P. R. Schreiner and B. M. Smarsly, *J. Mater. Chem. A*, 2020, **8**, 4107–4117.

9 X. Yu and C. T. Williams, *Catal. Sci. Technol.*, 2022, **12**, 5765–5794.

10 A. Trommer, J. Hessling, P. R. Schreiner, M. Schönhoff and B. M. Smarsly, *ACS Appl. Mater. Interfaces*, 2025, **17**, 24283–24299.

11 M. Nasrollahzadeh, N. Shafiei, Z. Nezafat, N. S. S. Bidgoli and F. Soleimani, *Carbohydr. Polym.*, 2020, **241**, 116353.

12 T. Chandy and C. P. Sharma, *Biomater. Artif. Cells Artif. Organs*, 1990, **18**, 1–24.

13 M. N. R. Kumar, *React. Funct. Polym.*, 2000, **46**, 1–27.

14 V. P. Santos, N. S. Marques, P. C. Maia, M. A. B. D. Lima, L. D. O. Franco and G. M. D. Campos-Takaki, *Int. J. Mol. Sci.*, 2020, **21**, 4290.

15 D. J. Macquarrie and J. J. Hardy, *Ind. Eng. Chem. Res.*, 2005, **44**, 8499–8520.

16 H. Zhang, H. Li, C. C. Xu and S. Yang, *ACS Catal.*, 2019, **9**, 10990–11029.

17 E. Guibal, *Prog. Polym. Sci.*, 2005, **30**, 71–109.

18 T. F. Jiao, J. Zhou, J. Zhou, L. Gao, Y. Xing and X. Li, *Iran. Polym. J.*, 2011, **20**, 123–136.

19 Á. Molnár, *Coord. Chem. Rev.*, 2019, **388**, 126–171.

20 Y. Lin, C. Kong and L. Chen, *RSC Adv.*, 2016, **6**, 32598–32614.

21 G. Anılır, E. Sert, E. Yılmaz and F. S. Atalay, *J. Solid State Chem.*, 2020, **283**, 121138.

22 J. Qiao, B. Zhang, X. Yu, X. Zou, X. Liu, L. Zhang and Y. Liu, *Inorg. Chem.*, 2022, **61**, 3708–3715.

23 I. W. Zapelini and D. Cardoso, *Microporous Mesoporous Mater.*, 2021, **324**, 111270.

24 M. Kostag and O. A. El Seoud, *Carbohydr. Polym. Technol. Appl.*, 2021, **2**, 100079.

25 N. Anbu, R. Maheswari, V. Elamathi, P. Varalakshmi and A. Dhakshinamoorthy, *Catal. Commun.*, 2020, **138**, 105954.

26 N. Anbu, S. Hariharan and A. Dhakshinamoorthy, *Mol. Catal.*, 2020, **484**, 110744.

27 S. M. Joseph, S. Krishnamoorthy, R. Paranthaman, J. Moses and C. Anandharamakrishnan, *Carbohydr. Polym. Technol. Appl.*, 2021, **2**, 100036.

28 B. Sakthivel and A. Dhakshinamoorthy, *J. Colloid Interface Sci.*, 2017, **485**, 75–80.

29 S. Zahedi, J. S. Ghomi and H. Shahbazi-Alavi, *Ultrason. Sonochem.*, 2018, **40**, 260–264.

30 V. K. Singh, K. Kumar, S. Rai, A. Chaudhary, K. Tungala and A. Das, *J. Environ. Chem. Eng.*, 2023, **11**, 110632.

31 L. Liang, L. Nie, M. Jiang, F. Bie, L. Shao, C. Qi, X. M. Zhang and X. Liu, *New J. Chem.*, 2018, **42**, 11023–11030.

32 H. Kayser, C. R. Müller, C. A. García-González, I. Smirnova, W. Leitner and P. D. de María, *Appl. Catal., A*, 2012, **445**, 180–186.

33 S. Deng, Y. Huang, E. Hu, L.-J. Ning, R. Xie, K. Yu, F. Lu, G. Lan and B. Lu, *Carbohydr. Polym.*, 2023, **321**, 121340.

34 D. Rani, P. Singla and J. Agarwal, *Carbohydr. Polym.*, 2018, **202**, 355–364.

35 A. Franconetti, P. Domínguez-Rodríguez, D. Lara-García, R. Prado-Gotor and F. Cabrera-Escribano, *Appl. Catal., A*, 2016, **517**, 176–186.

36 K. Rajender Reddy, K. Rajgopal, C. Uma Maheswari and M. Lakshmi Kantam, *New J. Chem.*, 2006, **30**, 1549–1552.

37 F. G. Bordwel and H. E. Fried, *J. Org. Chem.*, 1981, **46**, 4327–4331.

38 S. I. van Leuven and J. J. Kastelein, *Expert Opin. Pharmacother.*, 2005, **6**, 1191–1203.

39 B. D. Roth, *Prog. Med. Chem.*, 2002, **40**, 1–22.

40 B. D. Roth, C. Blankley, A. Chucholowski, E. Ferguson, M. Hoefle, D. Ortwine, R. Newton, C. Sekerke, D. Sliskovic and M. Wilson, *J. Med. Chem.*, 1991, **34**, 357–366.

41 ClinCalc DrugStats Database **https://clincalc.com/Drug Stats/Top300Drugs.aspx** (accessed July 2024).

42 H. Bonfante-Alvarez, G. De Avila-Montiel, A. Herrera-Barros, M. Torrenegra-Alarcon and A. D. Gonzalez-Delgado, *Chem. Eng. Trans.*, 2018, **70**, 1969–1974.

43 S. Komiya, T. Sone, Y. Usui, M. Hirano and A. Fukuoka, *Gold Bull.*, 1996, **29**, 131–136.

44 S. Liu, Y. Ni, J. Yang, H. Hu, A. Ying and S. Xu, *Chin. J. Chem.*, 2014, **32**, 343–348.

45 M. B. Ansari, H. Jin, M. N. Parvin and S.-E. Park, *Catal. Today*, 2012, **185**, 211–216.

46 A. R. Burgoyne and R. Meijboom, *Catal. Lett.*, 2013, **143**, 563–571.

47 S. Zhao, Y. Chen and Y.-F. Song, *Appl. Catal., A*, 2014, **475**, 140–146.

48 A. Erigoni, M. C. Hernández-Soto, F. Rey, C. Segarra and U. Díaz, *Catal. Today*, 2020, **345**, 227–236.

49 T. F. Machado, A. J. Valente, M. E. S. Serra and D. Murtinho, *Microporous Mesoporous Mater.*, 2023, **355**, 112561.

50 D. Jain, C. Khatri and A. Rani, *Fuel Process. Technol.*, 2010, **91**, 1015–1021.

51 S. K. Ma, J. Gruber, C. Davis, L. Newman, D. Gray, A. Wang, J. Grate, G. W. Huisman and R. A. Sheldon, *Green Chem.*, 2010, **12**, 81–86.

52 N. Andrushko, V. Andrushko, V. Tararov, A. Korostylev, G. König and A. Börner, *Chirality*, 2010, **22**, 534–541.

53 P. W. Woo, J. Hartman, Y. Huang, T. Nanninga, K. Bauman, D. E. Butler, J. R. Rubin, H. T. Lee and C. C. Huang, *J. Labelled Compd. Radiopharm.*, 1999, **42**, 121–127.

54 A. Ying, F. Qiu, C. Wu, H. Hu and J. Yang, *RSC Adv.*, 2014, **4**, 33175–33183.

55 WO2012145808, 2012.

56 A. Ying, Y. Ni, S. Xu, S. Liu, J. Yang and R. Li, *Ind. Eng. Chem. Res.*, 2014, **53**, 5678–5682.

57 Y. He, M. Li, L. Peng, T. Yang, D. Zhang and Y. Zhang, *ChemistrySelect*, 2024, **9**, e202304182.

58 K. C. Gupta and F. H. Jabrail, *Carbohydr. Polym.*, 2006, **66**, 43–54.

59 Y. I. Cho, H. K. No and S. P. Meyers, *J. Agric. Food Chem.*, 1998, **46**, 3839–3843.

60 J. Wang and J. Kinsella, *J. Food Sci.*, 1976, **41**, 286–292.

61 K. C. Gupta and M. R. Kumar, *Biomaterials*, 2000, **21**, 1115–1119.

62 P. T. Anastas and J. C. Warner, *Green Chem.*, 1998, **29**, 14821–14842.